Review article

Itia A. Favre-Bulle*, Alexander B. Stilgoe, Ethan K. Scott and Halina Rubinsztein-Dunlop

Optical trapping *in vivo*: theory, practice, and applications

https://doi.org/10.1515/nanoph-2019-0055
Received February 21, 2019; revised April 20, 2019; accepted May 1, 2019

Abstract: Since the time of their introduction, optical tweezers (OTs) have grown to be a powerful tool in the hands of biologists. OTs use highly focused laser light to guide, manipulate, or sort target objects, typically in the nanoscale to microscale range. OTs have been particularly useful in making quantitative measurements of forces acting in cellular systems; they can reach inside living cells and be used to study the mechanical properties of the fluids and structures that they contain. As all the measurements are conducted without physically contacting the system under study, they also avoid complications related to contamination and tissue damage. From the manipulation of fluorescent nanodiamonds to chromosomes, cells, and free-swimming bacteria, OTs have now been extended to challenging biological systems such as the vestibular system in zebrafish. Here, we will give an overview of OTs, the complications that arise in carrying out OTs *in vivo*, and specific OT methods that have been used to address a range of otherwise inaccessible biological questions.

Keywords: optical tweezers; scattering; microscopy; imaging; structured light; complex biological systems.

1 Introduction

The demonstration of optical forces in the early 1970s by Nobel laureate Arthur Ashkin [1, 2] led to the invention of optical traps or optical tweezers (OTs) 16 years later [3, 4]. One year after their introduction, OTs were used for the first time in biology when Ashkin demonstrated the manipulation of bacteria and viruses [5, 6]. He clearly demonstrated not only the three-dimensional trapping and manipulation of living organisms but showed that they survived and functioned normally after being trapped as well as after the trap was turned off. Shortly after, the first manipulations of cell organelles and chromosomes were carried out [7], which initiated and allowed for the precise investigation of cell's internal processes. Naturally, many studies of the thermal effects in OTs in biological environments followed these findings [8].

In general, molecules, cells, and biological tissues absorb light, which gives rise to localized and potentially harmful heating. A concern, therefore, is that the use of OTs could cause noxious heating or photodamage through the absorption of light. A possible solution to this problem has come from detailed studies of the optical properties of the biological matter [9], which have identified wavelength regions in which the absorption by biological tissue is minimized. We call such regions windows of transparency, and the most prominent one is in the infrared (IR) region for wavelengths between 700 and 1300 nm [8]. As a result, IR lasers are the tool of choice for most OT micromanipulation in biological systems [6].

OTs have now been widely employed in biology as a tool to actively probe, manipulate, and position biological systems or to measure mechanical properties from the nanoscale to microscale [10–15]. Highly focused laser light is able to deliver forces of the order of piconewtons and torques of the order of tens of piconewtons nanometers, which can be significant in the microscopic world. Such optical forces can stop and drag biological swimmers, such as bacteria, sperm, or microalgae [16–19]. It can slow down or even stop blood cells *in vivo* and consequently stop blood flow [20]. Forces of this magnitude can bend or stretch RNA and DNA, macromolecular assemblies such as microtubules or actin filaments [21–25], and even cell membranes or entire cells [26–29]. OT is also used to measure the mechanical properties of fluids such as their viscosity and elasticity and to study

***Corresponding author: Itia A. Favre-Bulle,** School of Mathematics and Physics, The University of Queensland, St Lucia, QLD 4072, Australia, e-mail: i.favrebulle@uq.edu.au. https://orcid.org/0000-0003-3118-356X
Alexander B. Stilgoe and Halina Rubinsztein-Dunlop: School of Mathematics and Physics, The University of Queensland, St Lucia, QLD 4072, Australia
Ethan K. Scott: School of Biomedical Sciences, The University of Queensland, St Lucia, QLD 4072, Australia; and Queensland Brain Institute, The University of Queensland, St Lucia, QLD 4072, Australia

wall effects or other complex surfaces and membranes [30–32].

Generally, OT is used to trap objects from 100 nm to 10 μm in size. It is difficult to trap transparent dielectric particles smaller than 100 nm, because the optical forces are small and Brownian motion is dominant. In contrast, trapping larger objects may require greater forces than can easily be generated with OTs because of inertia and gravity.

At the small end of the spectrum, nano-OTs would enable ultra-accurate measurements of the position of single nanoscale objects. In his seminal work [4], Ashkin established that, to achieve stable trapping, one has to create a potential depth of about 10 k_BT (where k_B is Boltzmann constant and T is temperature in Kelvin) to ensure the suppression of the particle's Brownian motion so that stochastic kick will not pull it out of the trap. It has been demonstrated that evanescent fields can be focused well beyond the diffraction limit to create traps of this depth [33–35]. This can be achieved using the plasmon nano-optics, where the metallic nanostructures support surface resonances and enable the control of light down to nanometer scales [36]. With plasmonic nanostructures, the light can surpass the diffraction limit and at the same time increase its confinement by increasing the depth of the trap. This provides new opportunities for optical traps at the nanoscale.

As mentioned above, at the other end of the scale for trapping is the limit of trapping large objects, above 10 μm using a single optical trap, as the optical forces available cannot create a gradient force large enough to enable 3D trapping and manipulation. However, there are many modified OT techniques that enable this sort of trapping and manipulation. One example is a reflection trap [37] that enables a highly controlled trapping of living organisms up to 50 μm in size. Another method for enhancing trapping forces and therefore trapping larger objects is the use of structured light, as structured light gives an order-of-magnitude higher trap stiffness than traditional Gaussian traps provide. The stiffness of such a trap can be an order of magnitude greater than the equivalent Gaussian trap and the signal-to-noise ratio is also strongly improved [38].

The use of OTs on the microscopic scale in the biological world enabled the investigation of a broad range of complex systems, phenomena, and processes. A unique advantage of the use of OTs in biology is that it is a noncontact method, where forces on the order of piconewtons can be applied very precisely *in vivo* and without any physical interaction, contamination, or damage. In addition, the information contained in the light used for optical manipulation can be used to quantify physical parameters such as forces, viscosity, and elasticity on exceptionally small scales and short timescales. Subsequent responses of any biological system to optical forces can be measured with very high precision – forces down to femtonewtons and displacements down to a single angstrom.

Recent comprehensive reviews on OTs have covered the physical theory and modeling of optical trapping [11, 39, 40], single-cell manipulation and mechanical characterization [29, 41], the biophysical analysis of single molecules [42, 43], and recent advances and possible future developments in the field [44–46]. In this current review, we focus on the application of OTs for the study of biology, ranging from molecules to macroscopic tissues. In discussing these methods, we will pay particular attention to innovative OT configurations that have permitted the manipulation of large objects and objects located in the highly scattering milieu of biological tissues.

2 How is light used to move, manipulate, and spin objects

OT is a noninvasive method for physical manipulation as it uses only the properties of light to apply forces on a large variety of objects from plastic materials, silica beads, living cells, and organelles, absorbing metal particles to polymer-based optically driven micromachine elements. By focusing a laser beam into a diffraction-limited spot, one can create an intensity gradient near the focus, drawing high refractive index transparent objects toward the focal point. However, when the refractive index of a trapped object is smaller than that of the surrounding medium, the object will be pushed away from the most intense part of the beam. The same will happen if we were to manipulate highly absorbing objects. The trapping principles and theory for a single beam optical trap (Figure 1A) depend on the object size relative to the wavelength of the laser beam λ, its refractive index, and the properties of the surrounding medium. The optical gradient force on large particles (in comparison to the wavelength of light used for trapping) can be calculated using ray optics. The particle, refracting light, would undergo a nonzero momentum transfer from the photons in the direction of the focused spot. When the diameter of a trapped particle is much smaller than the wavelength of light used for trapping, the particle can be treated as a point dipole in an inhomogeneous electromagnetic field and will follow the intensity gradient toward the center

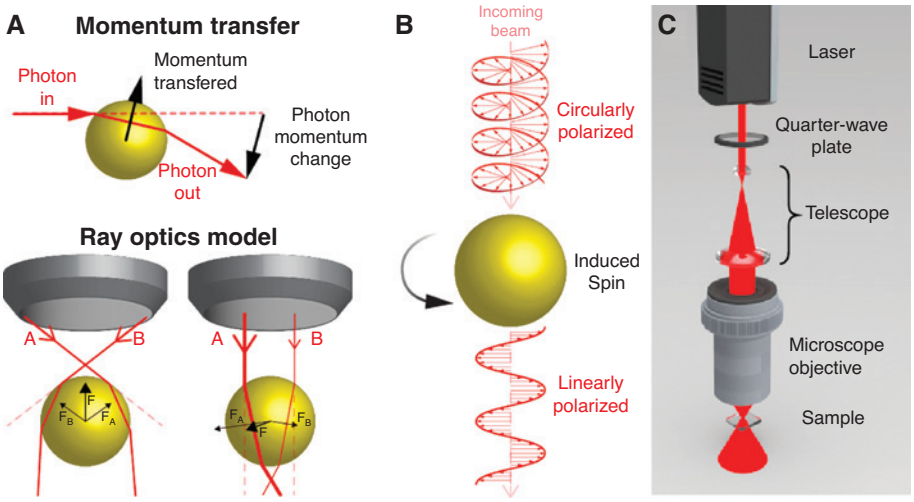

Figure 1: Manipulation of high refractive index transparent particles with light.
(A) Top: Sketch illustrating that the refraction of a photon within a particle induces a transfer of momentum to the particle. Bottom: Ray optics model for a focused beam and gradient force. (B) Transfer of angular momentum to a birefringent particle receiving a circularly polarized light and transmitting a linearly polarized light. (C) Basic experimental setup for OTs.

of the beam. Gradient forces on intermediate-sized particles (0.1–10 λ), however, cannot be calculated from the ray optics model or the point-dipole model, and a more complete electromagnetic field model is necessary for an accurate description of the force acting on the system in this intermediate-sized regime [47–49]. This is an important point as a vast majority of experiments lie in this size regime. The majority of theories deal with the trapping of spherical objects. In practice and especially in many of the biologically significant applications, the objects that are being manipulated are not spherical; therefore, consideration should be given to the shape and refractive index variations throughout the object [50–52].

The gradient force is not the only force that an object would be exposed to within an optical trap. Another force, known as the optical radiation pressure force [1], results from the absorption or the reflection of light by the object. Consequently, radiation pressure pushes the particle away from the center of the optical trap and therefore works against the gradient force [53–56]. For the gradient force to overcome the radiation pressure force, the particle has to be placed in a sufficiently strong intensity gradient. Such strong intensity gradients can be created using high numerical aperture (NA) objectives that can tightly focus laser beams down to a diffraction-limited spot. This permits the trapping of high refractive index transparent objects from hundreds of micrometers down to few nanometers [57] and create forces up to hundreds of piconewtons [4].

Light can also carry angular momentum. Circularly polarized light is an example of light with angular momentum. In this case, the electric field vector can be seen as spinning in a circle in the direction of light propagation and so carries $\pm\hbar$ per photon of spin angular momentum depending on the handedness of the spin. This spin angular momentum from the light can be transferred to an object exhibiting birefringence. Birefringent objects are optically anisotropic materials with a refractive index that depends on the polarization and propagation direction of the light they are exposed to. For example, a birefringent object would cause a relative delay in the electric field of circularly polarized light along orthogonal axes, potentially transforming this circularly polarized light into linearly or more generally to elliptically polarized light. This will optically induce a torque on the object as the total momentum of the system has to be conserved (see Figure 1B). Consequently, birefringent particles can be rotated with a constant angular speed determined by the optical torque created by the laser beam and the viscous drag from its surrounding acting on the particle. Speeds as fast as 2.45 MHz at a pressure of 1 Pa can be achieved where there is vastly diminished drag [58]. In more realistic environments, this technique is used to measure the viscous drag of the particle; consequently, the viscoelastic properties of biological fluids on the microscale can be determined.

An OT system can be constructed from a small number of optical elements comprising a laser beam followed by a couple of optics to steer and collimate the incoming beam and a microscope objective (or other high NA lens) to tightly focus the beam to create a single diffraction-limited spot to trap particles. The lasers that are commonly

used to produce linearly polarized light and so carry linear momentum of light that can then be transferred to the trapped objects. The simple addition of a quarter-wave plate in the laser path allows the transformation of linearly polarized light into circularly polarized light and therefore provide the beam with an angular momentum, which can be used to spin a target object, providing that its optical properties are right (see Figure 1C).

3 Quantitative measurements of forces and torques

As mentioned earlier, the force that OTs can apply on a small object is dependent on the intensity gradient of light [4] and is given by

$$F \propto -\nabla \left|E\right|^2,$$

where F is the force on the particle and E is the electric field of the incoming light. $\nabla|E|^2$, the gradient of light, can be approximated by $\nabla|E|^2 \simeq a + bx + \ldots$, where x is a small displacement. We thus obtain a relationship for optical force equivalent to the well-known Hookean spring model:

$$F \simeq F_0 - kx,$$

which consists of a constant force F_0 plus a change of force proportional to displacement. This expression holds and generalizes for many types of rigid larger particles as well [59]. Much of the literature is devoted to the quantification and the measurement of forces near the focus of the laser beam, or local equilibria, and in particular the determination of the local trap response constant (trap stiffness) k.

Usually, optical forces can be determined by measuring light emitted from the particle and a careful calibration of the optical trap. However, there is no simple way to measure optical forces that would be applicable to all sizes and shapes of trapped objects. Several methods have been developed to achieve just that, and each method has its own strengths, capabilities, and appropriate applications. The minimal apparatus for force detection is the trapping apparatus itself with the addition of the imaging system for the observation of the trapped particle, preferably at video rate or higher. The other main category of measurements is what could be called local probe measurement. These measurements are either based on the detection of the OT beam itself or using an additional laser beam with low output power so it does not trap the object. The additional laser only weakly influences the particle; thus, the light scattered can be a measure of the position of the trapped object in the small displacement limit. Measurements based on these techniques require the addition of extra optical elements downstream of the optical trap and may not be easily incorporated into existing complex OT systems such as those applying atomic force microscopy [60] or single-molecule fluorescence [61–63].

Some of the earliest force measurements in biological systems used escape force estimation [64, 65]. Both Block et al. and Ashkin et al. used video capture to calibrate and measure forces on biological particles. Block measured optical forces that induce a torque on bacterial flagellum [63] and Ashkin measured the force acting upon cellular organelles. Interestingly, in the Block et al. study, no calibration of the optical trap was needed as it relied on the return of the bacterium to its rotational equilibrium; thus, no uncertainties of the imparted optical forces were estimated.

There are a few physical parameters that must be assumed or measured before the calibration of the optical trap can be performed. Some of the "usual" assumptions, especially with the smaller and low-density objects within optical traps, are that the particle effectively moves with drag proportional to velocity at low Reynolds numbers [66]. In the Ashkin et al. experiment [65], a number of estimates of environmental contributions were made and a "maximum" estimated uncertainty of ≃140% was computed for the measurement of drag forces. However, this is a worst-case estimate, as environmental parameters such as the viscosity and changes of optical trap stiffness in cellular media were not well known at the time. Other experiments have used variants of this method and made reasonable estimates based on more controlled environmental conditions and more careful control of laser power [67–69].

In the linear (Hookean) spring regime, an optically trapped particle in water, or similar liquid, undergoes Brownian motion, which could potentially move the particle microns from its starting position over few seconds. Brownian motion is just as likely to move the particle toward or away from the equilibrium, but as the particle moves from the equilibrium the optical force increases, pushing it back to the equilibrium position with larger force. This behavior can be thought of in a similar way to a marble rolling inside a bowl. In the case of a linear force, the shape of this "bowl", known as the potential, is parabolic in every direction. Figure 2A depicts the Brownian motion of an optically trapped particle inside a potential represented by the shaded paraboloid. Figure 2B shows how the mean square displacement (MSD) of the particle [70] varies in two dimensions with time between measurements. The inset shows a series of the particle's position equivalent to

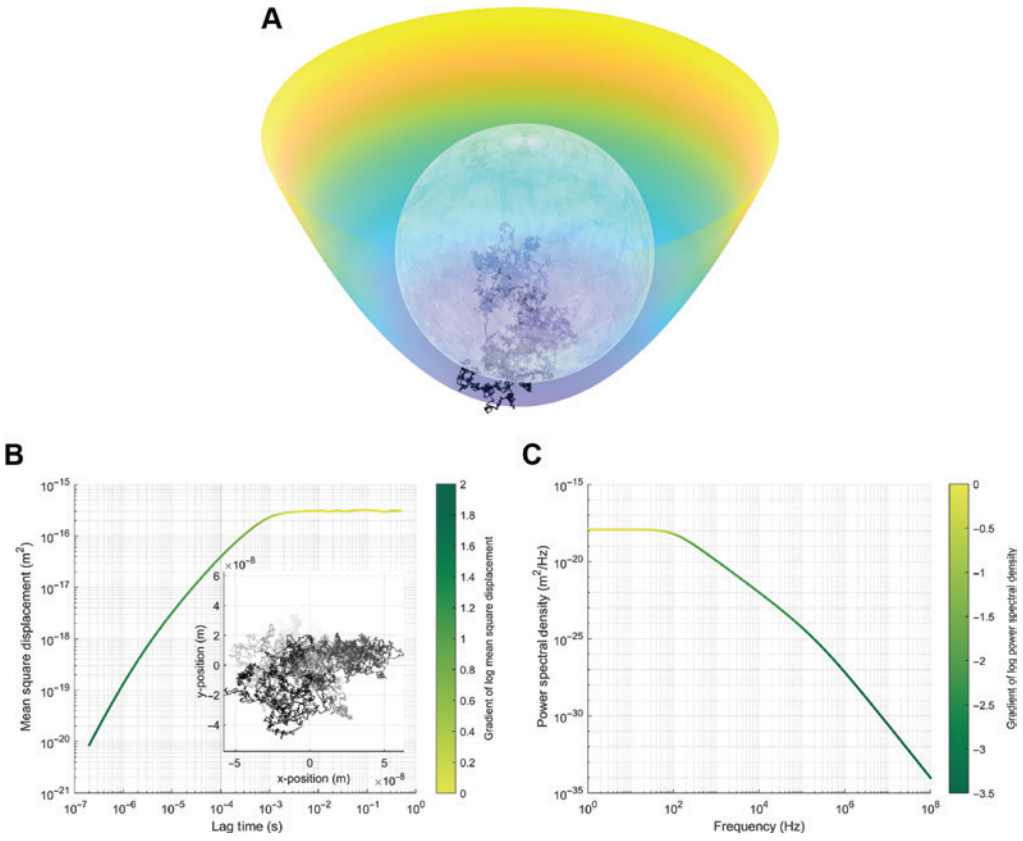

Figure 2: The confinement of an optically trapped particle.
(A) Visualization of a linear (Hookean) spring potential in 2D (shaded paraboloid) for an optically trapped particle moving under Brownian motion. (B) MSD and (C) power spectrum of a particle in linear OTs. In B, the Brownian motion of a trapped micron-sized particle is shown in the inset, with shading proportional to the latest sample point. In both B and C, the overdamped harmonic optical trap frequency response is represented by the lightest part of the curves. The Brownian motion of the particle can be resolved in the frequency spectrum and is represented by the middle section of the curves. The ballistic motion of the particle begins to be resolved at higher frequencies and is represented on the plot with the darkest shading.

40 ms of data. The MSD is used as a measure because the Brownian motion that drives the particle motion within the optical trap is completely random and thus will tend to a zero mean displacement as a length of the measurement increases. The curve in Figure 2B demonstrates that at short times the particle motion is dominated by the kicks of Brownian motion from the environment. As the time between the measurements is increased, the confinement by the OTs gives an upper limit to the excursion distance from the equilibrium position. As water constantly resists changing motions of the particle, the optical trap does not produce visible oscillations of the particle and without Brownian motion will settle at the equilibrium.

In the field of optical trapping, the power spectrum analysis of the position of a trapped object is an often used alternative to represent the data acquired and to calibrate OTs [71–73]. The power spectral density (power spectrum) of a time series describes how the trap strength varies and how strong it is. One practical model of OTs to consider, which describes the full power spectrum of a trapped particle, combines the Hookean spring model and a complete hydrodynamic model (Equation (5) of Ref. [73]). Using this model, we calculated the power spectrum of an ideal dataset of position data (Figure 2C). We will consider three characteristic features on this graph. The first feature is at low frequency, where the data are best fitted with a horizontal line, seen in the figure as a light yellow color. Within the model outlined here, this horizontal line corresponds to overdamped harmonic motion, a characteristic of optically trapped particles in the Stokes flow regime. As the frequency of motion is increased (Figure 1, light green region), the ability for the optical trap to control the motion relative to the instantaneous Brownian motion reduces. In this regime, it is still possible to resolve motion and measure physical processes acting on the particle, but when the other forces at these frequencies dominate the OTs act as a passive probe beam. Further increases of frequency (dark green region) cause the Stokes flow

approximation to break down and the hydrodynamic memory and ballistic character of motion to appear [73–76]. A combination of noise sources will typically limit measurements to about 100 kHz bandwidth, although this may in practice be a far lower frequency [73]. Model fitting with power spectrum calibration is a powerful technique to precisely characterize linear behavior when it can be assumed. These methods often use split detection such as a quadrant photodetector [77], balanced photodetector [75], or other types of split detector [78, 79] to detect the change in direction of the light scattered by the particle. Calibration using these methods requires several seconds of data capture to ensure a good fit to the model [80]. The timescale of practical OT measurements will determine if the apparatus is used to investigate the transport of large objects such as cells, organelles, and protein folding, which operate over minutes to milliseconds (Hz to kHz), or smaller, faster reactions such as enzyme turnover, molecular switching, and electron transfer in large molecules (kHz to MHz) [81–83].

Another method called direct force measurement has been used for decades [8, 84] but has only recently been clearly appreciated in a wider community outside of biochemistry [85, 86]. The idea is that optical forces for a transparent particle can be exactly determined by appropriate quantification of the light it scatters. Quadrant detectors cannot generally perform this operation, as they only weigh the intensity by the sign of the direction, e.g. the amount of light on one side of the detector versus the other. In contrast, a position-sensitive detector yields the position of the centroid of the light striking the detector. If we assume that the microscope imaging the light scattered by a transparent object obeys the Abbe sine condition, then its centroid is proportional to the angular displacement of the light scattered by the particle and transmitted by the microscope, and this observation permits force quantification. This method is very powerful, as it can be used to determine forces on nonspherical and deformable objects [50, 87]. It has some strict limitations of applicability due to the fact that the light collection angle of microscopes is limited and the light emitted and absorbed by the particle needs to be completely resolved for an exact determination of the force. It is not always necessary to use direct force measurement. It is possible to have small enough spherical particles that scatter reasonably well in all directions. Calibration can be performed such that forces in enclosed microscopic environments, such as inside cells, may be measured with quadrant photodiode [77, 88–90].

As mentioned earlier, the transfer of the angular momentum of light to particles is an important method of control and manipulation. Two kinds of angular momentum transfer can occur in OT: spin-angular momentum and orbital-angular momentum [91]. These two momentum transfers result in torque, the first one being on the particle axis causing it to spin on itself and the other on an arbitrary axis. They are measured in different ways. Spin-angular momentum is known as an intrinsic momentum, whose transfer is manifested and measured by the change of the light polarization [60, 70]. Orbital-angular momentum can be hard to measure because the change in torque needs to be quantified with respect to the distance to the axis of rotational motion [92]. There is no standard way of performing this measurement; it depends intimately on the physical distances and angle between the trapped handle and the object being measured. However, there are several methods for the measurement of orbital angular momentum, which with varying success measure this quite precisely the orbital angular momentum [93]. More indirect methods can also be used to measure the orbital angular momentum [94].

Torque measurements have few similarities to force measurements. Unlike linear momentum transfer, angular momentum transfer cannot be as unambiguously determined from the light scattered by the particle. Based on theory, one could argue that, to measure the electromagnetic angular momentum transfer, the field, and not just the intensity (as is the case with forces), needs to be known. However, the local linear torque acting on a particle can be deduced by looking at its rotation rate, provided the other external forces can be measured or computed from a priori information about the environment and is given by

$$\tau \simeq \tau_0 - \chi\phi$$

where τ is the torque acting on the particle, τ_0 is a constant torque, ϕ is the angle of the particle and χ is the rotational stiffness. Much of the literature involving the use of optical torques regards only the speed that a rotating object exhibits, usually to drive microfluidics, or generate flow fields. It may be the case that the measurement of optical torques appears less frequently in the literature due to the difficulties in controlling the location or orientation of the system being investigated so that an accurate measurement can be made.

Both absorbing [95] and birefringent transparent particles such as calcite [96], rods [97], nanorods [98], birefringent cylinders [99], vaterite [100], bespoke machines [101], and even molecules such as DNA [99, 102, 103] have optically measurable signs of angular momentum transfer.

The rotational torque due to the spin angular momentum transfer is [100, 104]

$$\tau_0 = \frac{\Delta\sigma P}{\omega}$$

where $\Delta\sigma$ is the change in spin angular momentum in the measurement channel, P is the laser power, and ω is the optical frequency. The choice of material is of particular importance as typical spherical glasses and or plastics are isotropic materials and only weakly interact with polarized light, therefore producing a hardly detectable angular momentum transfer. Strongly birefringent and transparent particles, such as calcium carbonate-based crystals, are great candidates. Interestingly, nonbirefringent particles such as cylinders, when their thickness is small enough, will experience torque transfer from both polarization and orbital angular momentum due to the phenomenon known as shape birefringence. The detection method for alignment torques and continuous spin angular momentum transfer from polarization use variants of a Stokes parameter measurement of various complexities (capability) due to how a particle is rotated [99, 100, 105].

Torque measurements have also been used for the measurement of forces or viscoelasticity properties of fluids and biological systems. If certain parameters, such as the viscosity surrounding a particle and the initial angular momentum imparted to the particle, are known, then the total torque on a spherical particle can be unambiguously measured [105]. In a study by Parkin et al., torque transfer from a beam carrying orbital angular momentum was determined by fitting a curve to opposite handed spin angular momentum contributions of a continuously rotating particle to the drag torque:

$$\tau_D = 8\pi\eta a^3\Omega$$

where η is the drag on the particle, a is the radius of the particle, and Ω is the particle rotation rate. Practically, it means that the change in polarization on the object exposed to the laser beam is measured for three different input polarization states. The orbital angular momentum transferred to the particle can be deduced from these measurements if we assume that spin and orbital angular momentum can be added.

The viscoelasticity of fluids can be measured through the measurement of torques acting on particles in the fluid [32, 106]. Bennett et al. and Zhang et al. applied an optical torque to a particle and measured its angular frequency and variation of the spin angular momentum transfer using polarization. Due to the reasonably spherical shape of the probe particles used, the rotational Stokes drag is used as a basis for analyzing the data and deducing the viscoelastic properties of the fluid. The measurement of viscoelastic properties of fluids *in vivo* is challenging due to the difficulty of precise calibration in a living organism. However, it is worth noting that recent studies have successfully measured the viscosity of fluids and elasticity of cells *in vivo* using an optical trapping technique [107, 108], opening new avenues for the study of mechanobiology *in vivo*.

4 Common applications of optical trapping in biology

The physical and chemical studies of biological materials were used to be performed in bulk, giving only an average measurement of stresses and strains occurring in the experiments. By providing measurement, analysis, and quantification at the nanoscale to microscale, OT has allowed studies at the level of individual molecules *in vivo*, vastly improving our understanding of the physical forces at play in living cells.

4.1 Single molecules

On the nanoscale, at the level of single molecules, OTs have been applied to a wide range of molecular motors [64, 109–117] as well as RNA, DNA [21, 118], and proteins [22, 119–122]. This has overcome the technical difficulties related to measuring movements of single molecules, as their motions occur on the length scale of angstroms to nanometers and on the timescale of milliseconds and shorter. However, their functions are essential and must be investigated to understand the basic functioning of any living organism.

One area in which OTs have allowed significant progress is the study of molecular motors and intracellular trafficking. Molecular motors are abundant in all living cells with a wide variety of roles and functions. They are responsible for DNA replication, RNA transcription, and protein synthesis. They drive cell division, induce cell motility, intracellular trafficking, and ciliary function. Molecular motors are known to be extremely energy efficient and have therefore been studied intensively. To obtain high spatial and temporal resolution of their behavior, a common method is to attach microscopic beads on those molecules and observe, manipulate, and measure forces on those beads with OTs when the motor is working [109, 110, 123, 124].

Rotary motors, such as bacterial flagellum, have been manipulated indirectly with OT. Originally, Block et al.

showed in 1989 that OT allows the measurement of the elastic properties of individual flagella. This sets the stage for more detailed analyses of the motor structure [125–127] and the forces required to induce movement [128]. More recently, Darnton and Berg [129] have made a detailed study of flagellum geometry and stiffness using OT based on the 12 helical states, or polymorphic forms, predicted by Calladine [130, 131].

Another class of molecular motors, the linear motors, comprise kinesin and dynein, two molecules able to walk on microtubules but in opposite directions. These are essential to the transport of materials in cells. The mechanochemical processes underlying this transport have been extensively studied *in vitro*, and OT played a crucial role in these investigations. OT allowed measurements of the forces exerted in the process of microtubules growth, their stiffness, as well as the binding mechanics of motor proteins on the filaments [25, 113, 132]. Combining OT with dual beam interferometry, Svoboda et al. demonstrated that stepwise character of the kinesin molecule's motion, measuring the nanometer-scale displacements and piconewton forces produced [123]. The measured average step size of 8 nm shows the incredible sensitivity of the method. This study revealed the hand-over-hand walking behavior of kinesin along microtubules and therefore led to a deeper understanding of this complex protein and the cellular trafficking that it delivers.

OTs have also been applied to the study of DNA [21, 22, 114, 118, 122, 133–138], where it provides unique features for exploring the DNA's structure and interactions with proteins. For example, Bustamante's group presented a study designed to characterize the rotation and translocation of the DNA being packaged by the motor throughout the entire range of capsid filling. This was enabled by the unique properties of OTs to be able to hold the motor part of the structure and analyze the rotation of the DNA when it was packaged into the motor. They were able to show that the motor rotates the DNA during packaging [139].

In another study, DNA bundles have been attached to microbeads and stretched using OT, revealing the DNA elasticity, the forces involved with transcription and packaging, and its different helical forms. More recently, nanomachines, or artificial DNA-based devices, have been designed to exploit the mechanical nature of the DNA double helix and generate forces and torques [140–143].

4.2 Single-cell manipulation

Within every cell, a range of organelles make specific contributions to the cell's overall structure and physiology. Nuclei, mitochondria, and chloroplasts have been optically manipulated inside cells, providing information about their transport properties and processes, viscoelastic properties, and stress relaxation [65, 144–146]. Vesicles, which are lipid bilayer membranes containing a range of possible cargos, have been trapped in various cell types *in vivo* [147–150], and this work has been important in studying the architecture of their membranes [151]. Cell membranes are complex systems as they allow cell flexibility and elasticity as well as mediate and modulate signaling, trafficking, and permeability. Vesicles offer a simplified version of the cell membrane, permitting the analysis and visualization of their individual characteristics and components. Past studies provide the modeling and precise measurement of mechanical and rheological properties of vesicle membranes using OTs and show their high dependence on temperature [152, 153]. In addition, a cell or vesicle in a fluid imposes a hydrodynamic drag on neighboring objects but also to its own motion. Understanding this phenomenon led to the study of the hydrodynamic interactions on complex surfaces and its measurement and modeling [30].

From the nanomechanical characterization of membrane mechanics, cell division, cell-cell interaction, cell motility and migration to *in vitro* fertilization, single-cell transfection, or tissue engineering, the examination of how individual cells operate, function, and interact with each other is currently helping to reveal invisible processes and communication and elucidate subcellular processes and population behavior.

The most popular application of OT for single-cell manipulation is to confine and position cells in a static or dynamic flow environment. This includes cell sorting and the study of cell motility and swimming.

Cell sorting was originally demonstrated by Buican et al. in 1987 when they created a trap with two weakly focused counterpropagating beams, selected cells with particular optical properties, and transported them reliably over millimeter distance [154]. This groundbreaking work led to the development of other active sorting techniques using single or multiple traps based on fluorescence activation [155, 156], magnetic activation (magnetic activated cell sorting) [157], or simple cell imaging identification [158–160]. In parallel, passive optical sorting techniques have been developed based on the identification of cells on their shape, size, and refractive index difference, avoiding the use of markers and keeping cells intact, in their original state [161, 162].

Conveniently, OTs can hold moving microorganisms such as swimming bacteria, parasites, sperm, or microalgae and allow the quantification of their swimming

forces and their interaction with the surroundings. The swimming force, or thrust force, can be calculated from the measurement of the distribution of position of the organism in the trap but also by measuring the minimum laser power needed to hold a swimmer in the trap, as this is directly proportional to the swimmer's swimming force. Based on these methods, multiple studies have used OTs to quantify swimming thrust and torque for a wide range of swimmers. Chattopadhyay et al. investigated the forces and torques of *Escherichia coli* using OT to study their behavior when they were exposed to an external flow [163]. By looking at the power spectrum of the position of *E. coli* in the trap, they were able to visualize directly the two frequencies associated with the angular velocities of the cell body Ω and the flagella bundle ω. They reported that the average frequency values, calculated from more than 200 bacteria to be 19.6 ± 0.3 Hz for the body and 115 ± 2 Hz for the flagella bundle, which agree with previous measurements based on imaging [164, 165]. In addition, they were able to measure the average thrust of *E. coli* to be 0.57 pN and the average torque 5×10^{-19} N m, revealing the precise measurements of bacterial propulsion using OT. In the work of Armstrong et al., OTs were used to characterize the swimming and tumbling behavior and the clear characterization of those motions was determined. More importantly, the viscous forces were determined and linked to polymorphic changes of the flagella [166].

The application and measurement of forces on single cells have also been useful for studies of cell-cell interactions, cell migration, cell division, and the cells' mechanical properties. The characteristics of the mechanical deformation of living cells are known to strongly influence their functions, and their inability to deform sufficiently can contribute to a number of diseases. Red blood cells (RBCs) are a good example of cells whose shape flexibility is essential to the organism and its function. Their average diameter is about 8 μm, but they deform to fit through capillaries as narrow as 3 μm in diameter. In a study by Dao et al. in 2003, they attached two silica microbeads onto an RBC's surface, pulled those beads in opposite directions with two optical traps, and generated impressively large deformations of the cell with optical forces as large as 600 pN. By modeling and measuring those deformations, they revealed the key viscoelastic properties of the cell membrane and captured the complete deformation characteristics of the cell [26].

Blood transfusions require high RBC survivability, leading to strict rules for the blood's storage. This precise cell characterization and its linkage with health and survivability are therefore of great importance for medicine. In Kashchuk's work [167], dual OTs were used to controllably stretch blood cells of different ages and measure their stiffness. Measurements were done by holding one trap at a constant position and stretching the cell by moving the other trap away from the first trap. Using this method, the modulus of deformation could be precisely measured. This work could potentially help to choose the fittest RBCs for longer-term storage and blood transfusions.

4.3 Advanced devices and optical techniques for OT in biology

Given the flexibility of OT and the diverse biological questions that it can address, a wide range of techniques and OT systems, based on the core system described in Figure 1C, have been developed and implemented in biological experiments [168–170].

The most common mode of operation for OT is to use a highly focused Gaussian beam for trapping. However, when we want to dynamically manipulate several objects at once or if the trapping is to be done on a large objects, multiple highly focused laser beams are required to grab the cell at several points and manipulate it. To enable this, either multiple independently controllable lasers or beam multiplexing, shaping, and or scanning needs to be incorporated into the apparatus.

For example, the use of holograms or other types of diffractive optical elements have significantly extended the possibilities for optical trapping and manipulation. By placing a diffractive optical element in the sample's conjugate plane, one can produce the desired intensity and phase profile of light at the sample plane. Fixed holograms can be generated using photolithographic techniques and can produce fixed optical traps at arbitrary locations. However, very often, the study of biological systems requires the dynamic control of OTs, and this can be achieved using either fast scanning devices, such as acousto-optic deflectors and galvo mirrors, or spatial light modulators (SLM), such as deformable mirrors, digital micromirror device, and liquid crystal SLM. With scanning devices, high scanning speeds can be reached, allowing the generation of multiple optical traps by time sharing. In addition, they are usually formed in only one- or two-axis planes due to a lack of capability to easily refocus the incident laser beam. SLMs can alter the wavefront of the laser, and provided sufficient resolution can allow multi-beam generation without time sharing. However, this increased flexibility can slow operation in some cases due to the factors, including the complexity of the calculation of the display pattern and the speed at which pixels switch values.

The approaches and devices mentioned above provide several ways to deliver multiple, arbitrarily shaped, dynamically controlled optical traps. One example of the combination of optical systems and devices developed for multiple particle trapping is known as holographic OTs (HOTs). Originally demonstrated with diffractive optical elements [171], HOTs have now been designed with SLMs enabling dynamic optical manipulation [172].

When we are interested in both the physical and chemical properties of the trapped microscopic objects, we can combine trapping with other imaging or spectroscopic techniques. In particular, if the aim is to characterize physical and chemical properties and the temporal evolution of a single cell, for example, this characterization can be done with Raman tweezers, a technique that combines Raman spectroscopy as a diagnostic tool and OTs for single-cell trapping and manipulation [173, 174]. In yet another study, a micro-Raman spectrometer was combined with external OTs enabling resonance Raman studies of a single functional trapped cell. The advantage of this particular experiment was that two separate lasers were used for the two functions of the setup – separate lasers for trapping and the Raman spectrometry. This configuration enabled separate wavelengths and powers to be used for these two functions [175]. Specific applications of Raman tweezers include the analysis of cancer cells, microorganisms, subcellular structures, and organelles such as chromosomes and mitochondria. Single-cell interrogation using the powerful combination of OTs and chemical analysis with Raman spectroscopy brings the potential advantages of spectroscopic identification of cellular components with high spatial resolution, but foremost this technique gives the freedom from intercellular and surface adhesion effects on the single-cell level.

Another example of a very powerful combination is the integration of OTs in fluorescence resonance energy transfer spectroscopy (FRET). Such systems have been used for studies on how the mechanical environment influences cell population functions, in once case exploring the phenomenon of how mechanical stimuli are transmitted into biochemical signals. The cell was stimulated using OTs that exerted a known adhesion force and mechanotransduction was studied using FRET [63].

The final example of a powerful combination of OTs with other spectroscopic techniques is the work done by Käll's group. They demonstrated that, using OTs to move a single silver nanoparticle into a contact with an immobilized particle, an isolated surface-enhanced Raman spectroscopy (SERS) active silver particle dimer was formed. As the dimerization occurred, the SERS intensity was enhanced by a factor of approximately 20 [176].

These new combinations of OT with complementary optical methods, and the resulting advances, have allowed the investigation of a wide variety of complex biological systems from the nanoscale to the microscale.

5 Trapping at the limits

5.1 Light scattering in biology

OT, like any optical technique, has its challenges. In the context of the manipulation of biological systems, delivering light to specific regions, to either manipulate or simply illuminate, can be a difficult task. OT is challenging *in vivo* both because of the absorption of light by biological tissue and from the scattering of the light when it encounters refractive index surfaces [177]. The disparity of refractive indices within a cell or biological tissue is enormously complex and dynamic, as cells and their organelles are tightly packed and in constant motion. As you go deeper into a biological tissue, spatial light distortions increase, leading to the random speckle pattern of the incoming illumination (see illustration in Figure 3A) and a defocusing of targeted light.

Despite those difficulties, direct optical manipulation is possible within low absorptive or low scattering environments such as shallow tissue regions and transparent model systems. In such situations, trapping can be performed *in vivo* without the need to compensate for light scattering and distortions. Blood cells have been manipulated and trapped *in vivo* in mice [20] in shallow regions of the ear (~40 μm deep), allowing the measurement of the drag force of the blood flow circulating around the cell. At such depths, forces applied on circulating RBCs are sufficient to pause the motion of the cell and completely block blood flow in thin blood vessels. Similarly, nanoparticles and microparticles and cells have been manipulated in genetically engineered transparent zebrafish [107, 178, 179], a relatively small model compared to mice. Zebrafish are of great interest due to its advanced brain structure and its small dimensions [180, 181]. The transparency of this relatively new model facilitates light transmission and therefore allows optical manipulation deeper in tissue. Blehm et al. reported trapping down to 500 μm in such a model [107]. In this work, they performed the first rheological characterization *in vivo* in a vertebrate with great impact for biomedicine. The method they used was introduced as "active microrheology by optical trapping *in vivo*" and used OT as a unique tool allowing the measurement of physical properties of cells *in vivo* on the microscale deep

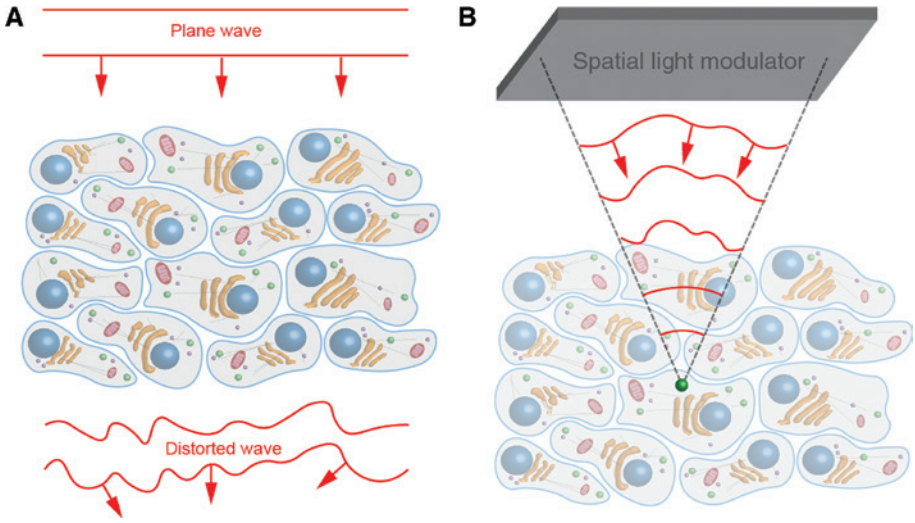

Figure 3: Scattering in tissue.
(A) Illustration of light distortion through biological tissue. (B) Illustration of light wavefront shaping with an SLM aiming to optically manipulate an organelle within biological tissue.

within the organism. As the physical properties of tissue and in particular the matrix elasticity of a cell can determine the development of cancer or other malignant phenotype, this method has the potential to allow the direct detection of abnormal transformation of cells *in vivo* and is therefore of great interest for medical sciences.

As discussed in Section 3, the measurements of forces or torques usually require calibration of the optical trapping system. Different methods for *in vivo* calibration have been developed such as the light-momentum change method, the microrheology method, or the refractive index matching method. A comprehensive study comparing these methods favored the momentum-change approach, as it requires just a single calibration and is insensitive to changes such as the refractive index in the surroundings and changes in the geometry of the particle itself [182]. However, depending of the application, a careful consideration of all these methods is recommended.

5.2 Trapping through highly scattering media

Understanding and predicting light scattering in complex media is necessary for the precise delivery of light through it. However, the distribution, movements, and interactions of molecules, organelles, and even cells are hardly predictable. Therefore, the study and modeling of the scattering properties of biological tissues is a rich and timely area of research. The principles and fundamentals of light scattering [183] have been covered in a number of books and review articles as well as the various models for biological tissue [184–186].

Recent advances in the field and the surge of new imaging techniques and light shaping devices have allowed imaging and manipulation ever deeper in highly scattering media, including biological tissues [187, 188]. The approach behind these methods is to create arbitrary light illumination, correcting for light distortions originating from both the sample and the optical system (see illustration in Figure 3B).

The generation of arbitrarily shaped wavefronts has been of great interest to both biologists and physicists, and nowadays, delivering light into one plane of a sample is relatively straightforward. Any arbitrary 2D surface can be generated using techniques such as Gerchberg-Saxton [189] or with prisms and lenses [190]. The Gerchberg-Saxton algorithm is of particular interest in optogenetics and neuroscience. This method used for 2D light shaping relies on the iterative calculation of a hologram in the Fourier plane of the sample to create a chosen illumination pattern within the sample. It retrieves the phase of both the incoming light distribution (usually a Gaussian profile incoming beam) and the target intensity profile related via the Fourier transform. One limitation of this method is the poor axial resolution, or the significant axial spreading of the light, when illuminating large 2D regions. However, the use of a two-photon laser and its combination with a grating to perform temporal focusing, as described by Emiliani's group [191, 192], allows a remarkable confinement of the light in the plane of illumination.

In 3D, however, light shaping is more nuanced. Simple 3D illumination patterns, such as multiple spots, have been achieved and proven to be useful for optical trapping [172, 193] and optogenetics [194, 195]. However, 3D surfaces

are challenging to create in nonturbid media [196] and are not sufficiently robust for their implementation in biology.

Čižmár et al. demonstrated for the first time the *in situ* wavefront correction for optical trapping through highly turbid media [197, 198]. Using an SLM, they altered and optimized the phase of the modes composing the incoming beam such that they could interfere constructively at the trap location. Interestingly, this method provides correction for not only aberrations from the sample but also the entire optical train, starting at the laser output and ending at the trap focus.

Other methods for wavefront correction *in vivo* include the use of a "guidestar" [199]. Recent work shows that a micrometer-sized focal spot deep within tissue can serve as a guide for the calculation of the optical properties of the medium and the needed corrections to get a tightly illuminated spot deep within tissue. Coupled with feedback loops and fast detectors and modulators, Bloch et al. showed that the fast correction of focused light in dynamic samples is feasible at speeds up to 4.1 kHz [200]. These great advances are promising for fields such as optogenetics, drug delivery, and deep tissue imaging.

5.3 Trapping complex biological objects and structures

As the manipulation of large objects is challenging due to their large geometry and inertia, additional light shaping techniques have been developed to optimize and increase optical trap stiffness [37, 38]. Taylor et al. designed a structured incident light field able to interact with large particles, as a particle acting as a beam splitter would with a Gaussian beam, and thereby increased previously achieved trapping stiffness by more than 20 times for 3.5 to 10 µm silica particles. Another interesting example comes from Pitzek et al., who used an optical mirror trap. In addition to a normal optical trap, they introduce a secondary trap that reflects on the sample chamber surface to reach and trap the particle from the back and therefore propagates in the opposite direction to the primary trap, thus enhancing the trap stiffness. This technique allows work with long working distance, large field of view, and low NA microscope objectives to manipulate particles up to 45 µm.

Kirkham et al. used a variant of HOT to position and organize different cell types into 3D structures, allowing them to bond and stabilize [201]. As HOTs can create multiple independent traps in 3D, other studies have shown experimentally how one or multiple cell types can be assembled in specific structures to mimic real biological tissue and therefore produce complex synthetic tissues [202, 203].

These optical trapping designs are flexible and offer a high degree of control but remain challenging to implement in biological systems; therefore, very few studies report the optical manipulation of large objects in biology.

Using a simpler approach, we have targeted and manipulated the otoliths in live zebrafish. Otoliths or earstones are calcium carbonate crystals located in the ears

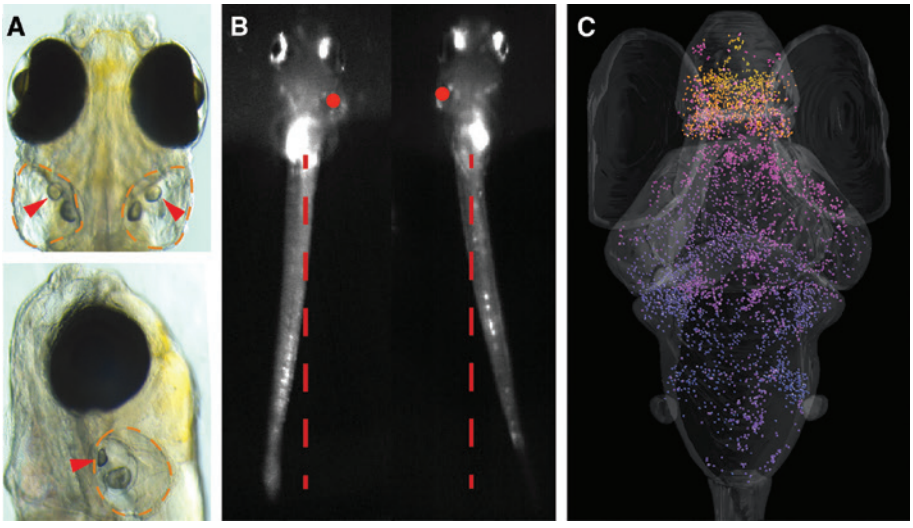

Figure 4: Manipulating zebrafish inner ear with OT.
(A) Top view (top) and side view (bottom) of zebrafish. The inner ear is circled in dashed orange. Acceleration sensing otolith pointed in red. (B) Tail bend in response to single otolith exterior trapping (red dot). The original position of the tail is shown in dashed red line. (C) Distribution of neuronal intensity profiles in the brain (see details in Ref. [204]). Credit to Gilles Vanwalleghem and Nick Valmas.

of zebrafish, and their movements permit vestibular and auditory perception. Otoliths are typically about 55 μm in diameter in 6 days post-fertilization fish and are located about 150 μm deep in tissue (Figure 4A). Despite the obstacles stemming from otolith location and geometry, we showed in a recent study [204, 205] that we can successfully apply forces to the otolith responsible for acceleration sensing and thereby simulate acceleration without physically moving the animal. Previous studies on the vestibular system involve accelerating or spinning the animal, introducing difficulties in imaging or unwanted artifacts such as water flow in the case of zebrafish [206–208]. The introduction of OT for the manipulation of the inner ear also allows a specific stimulation of a single otolith, which could not be obtained with motion of the animal as well as both otoliths simultaneously, therefore simulating more natural movements. Using this method, we determined that the behavioral responses (from eyes and tail) to the simultaneous manipulation of both otoliths was the linear combination of the behavioral responses to single otolith manipulations (Figure 4B).

Further investigation of the information processing and neuronal network of the vestibular system, from the otolith to the tail and eyes, led us to image the brain activity in response to various OT manipulation [205]. Such imaging relied on the animal's stability, so our ability to simulate movement without physically moving the animal was key. Our technique allowed us to simulate various acceleration amplitudes and directions, revealing the brain activity that resulted from the perceived acceleration (Figure 4C). These results and this new application of OT open the door to many further questions related to the perception and sensory processing of vestibular and auditory stimuli.

6 Summary

The demonstration of optical trapping and precise manipulation of biological systems by Ashkin triggered an unprecedented investigation of biological phenomena from molecular interactions and behavior to a whole organ function. In parallel with these investigations, the precise quantification of forces and torques has been very useful for studies of the mechanobiology of molecules, cells, and tissues, all of which would have been extremely difficult without the noncontact forces provided by OT. In combination with subsequent developments in arbitrary light shaping, OT has been enhanced, optimized, and extended to manipulate and measure a large variety of objects *in vivo*. Experiments and studies using OT will continue to benefit from technological improvements that will increase their power, depth, and precision and will continue to make profound contributions to our understanding of biological molecules, cells, and tissues.

Acknowledgments: Support was provided by an ARC Discovery Project (DP140100753) to H.R.-D. and a fellowship from the Human Frontiers Science Program (LT000146/2016). Further support was provided by an NHMRC Project Grant (APP1066887), ARC Future Fellowship (FT110100887), a Simons Foundation Pilot Award (399432), and two ARC Discovery Project Grants (DP140102036 and DP110103612) to E.K.S.

References

[1] Ashkin A. Acceleration and trapping of particles by radiation pressure. Phys Rev Lett 1970;24:156–9.
[2] Ashkin A, Dziedzic JM. Optical levitation by radiation pressure. Appl Phys Lett 1971;19:283–5.
[3] Ashkin A. History of optical trapping and manipulation of small-neutral particle, atoms, and molecules. IEEE J Sel Top Quantum Electron 2000;6:841–56.
[4] Ashkin A, Dziedzic JM, Bjorkholm JE, Chu S. Observation of a single-beam gradient force optical trap for dielectric particles. Opt Lett 1986;11:288–90.
[5] Ashkin A, Dziedzic JM. Optical trapping and manipulation of viruses and bacteria. Science (NY) 1987;235:1517–20.
[6] Ashkin A, Dziedzic JM, Yamane T. Optical trapping and manipulation of single cells using infrared laser beams. Nature 1987;330:769–71.
[7] Berns MW, Wright WH, Tromberg BJ, Profeta GA, Andrews JJ, Walter RJ. Use of a laser-induced optical force trap to study chromosome movement on the mitotic spindle. Proc Natl Acad Sci USA 1989;86:4539–43.
[8] Svoboda K, Block SM. Biological applications of optical forces. Annu Rev Biophys Biomol Struct 1994;23:247–85.
[9] Steven LJ. Optical properties of biological tissues: a review. Phys Med Biol 2013;58:R37.
[10] Dienerowitz M, Mazilu M, Dholakia K. Optical manipulation of nanoparticles: a review. J Nanophotonics 2008;2:021875.
[11] Padgett M, Bowman R. Tweezers with a twist. Nat Photonics 2011;5:343.
[12] Greulich KO. Manipulation of cells with laser microbeam scissors and optical tweezers: a review. Rep Prog Phys 2016;80:026601.
[13] Daly M, Sergides M, Nic Chormaic S. Optical trapping and manipulation of micrometer and submicrometer particles. Laser Photonics Rev 2015;9:309–29.
[14] Bui AAM, Stilgoe AB, Lenton ICD, et al. Theory and practice of simulation of optical tweezers. J Quant Spectrosc Radiat Transfer 2017;195:66–75.
[15] Zhang S, Gibson LJ, Stilgoe AB, Nieminen TA, Rubinsztein-Dunlop H. Measuring local properties inside a cell-mimicking structure using rotating optical tweezers. J Biophotonics e201900022.

[16] Juarez-Alvarez BA, Garces VG, Cordero-Esquivel B, Spalding GC, O'Donnell K. Studies of biflagellated microalgae adhesion using an optical trap system. Proc. SPIE 10723, San Diego, CA, USA, Optical Trapping and Optical Micromanipulation XV, 107231H, 7 September 2018.
[17] Pilat Z, Jezek J, Sery M, Trtilek M, Nedbal L, Zemanek P. Optical trapping of microalgae at 735–1064 nm: photodamage assessment. J Photochem Photobiol B Biol 2013;121:27–31.
[18] Nascimento JM, Botvinick EL, Shi LZ, Durrant B, Berns MW. Analysis of sperm motility using optical tweezers. J Biomed Opt 2006;11:044001.
[19] Min TL, Mears PJ, Chubiz LM, Rao CV, Golding I, Chemla YR. High-resolution, long-term characterization of bacterial motility using optical tweezers. Nat Methods 2009;6:831.
[20] Zhong M-C, Wei X-B, Zhou J-H, Wang Z-Q, Li Y-M. Trapping red blood cells in living animals using optical tweezers. Nat Commun 2013;4:1768.
[21] Allemand JF, Bensimon D, Croquette V. Stretching DNA and RNA to probe their interactions with proteins. Curr Opin Struct Biol 2003;13:266–74.
[22] Heller I, Hoekstra TP, King GA, Peterman EJG, Wuite GJL. Optical tweezers analysis of DNA-protein complexes. Chem Rev 2014;114:3087–119.
[23] Kerssemakers JWJ, Laura Munteanu E, Laan L, Noetzel TL, Janson ME, Dogterom M. Assembly dynamics of microtubules at molecular resolution. Nature 2006;442:709.
[24] Felgner H, Frank R, Schliwa M. Flexural rigidity of microtubules measured with the use of optical tweezers. J Cell Sci 1996;109:509–16.
[25] Footer MJ, Kerssemakers JWJ, Theriot JA, Dogterom M. Direct measurement of force generation by actin filament polymerization using an optical trap. Proc Natl Acad Sci USA 2007;104:2181–6.
[26] Dao M, Lim CT, Suresh S. Mechanics of the human red blood cell deformed by optical tweezers. J Mech Phys Solids 2003;51:2259–80.
[27] Ashkin A, Dziedzic JM. Internal cell manipulation using infrared laser traps. Proc Natl Acad Sci USA 1989;86:7914–8.
[28] Nussenzveig HM. Cell membrane biophysics with optical tweezers. Eur Biophys J 2018;47:499–514.
[29] Zhang H, Liu K-K. Optical tweezers for single cells. J R Soc Interface 2008;5:671–90.
[30] Zhang S, Gibson LJ, Stilgoe AB, Nieminen TA, Rubinsztein-Dunlop H. Impact of complex surfaces on biomicrorheological measurements using optical tweezers. Lab Chip 2018;18:315–22.
[31] Gibson LJ, Zhang S, Stilgoe AB, Nieminen TA, Rubinsztein-Dunlop H. Active rotational and translational microrheology beyond the linear spring regime. Phys Rev E 2017;95:042608.
[32] Bennett JS, Gibson LJ, Kelly RM, et al. Spatially-resolved rotational microrheology with an optically-trapped sphere. Sci Rep 2013;3:1759.
[33] Vigoureux JM, Courjon D. Detection of nonradiative fields in light of the Heisenberg uncertainty principle and the Rayleigh criterion. Appl Opt 1992;31:3170–7.
[34] Novotny L, Hecht B. Principles of nano-optics. Cambridge, UK, Cambridge University Press, 2012.
[35] Juan ML, Righini M, Quidant R. Plasmon nano-optical tweezers. Nat Photonics 2011;5:349.
[36] Schuller JA, Barnard ES, Cai W, Jun YC, White JS, Brongersma ML. Plasmonics for extreme light concentration and manipulation. Nat Mater 2010;9:193.
[37] Pitzek M, Steiger R, Thalhammer G, Bernet S, Ritsch-Marte M. Optical mirror trap with a large field of view. Opt Express 2009;17:19414–23.
[38] Taylor MA, Waleed M, Stilgoe AB, Rubinsztein-Dunlop H, Bowen WP. Enhanced optical trapping via structured scattering. Nat Photonics 2015;9:669.
[39] Ashkin A. Optical trapping and manipulation of neutral particles using lasers. Singapore, World Scientific, 2006, 940.
[40] Timo AN, Vincent LYL, Alexander BS, et al. Optical tweezers computational toolbox. J Opt A Pure Appl Opt 2007;9:S196.
[41] Karl Otto G. Manipulation of cells with laser microbeam scissors and optical tweezers: a review. Rep Prog Phys 2017;80:026601.
[42] Hormeño S, Arias-Gonzalez JR. Exploring mechanochemical processes in the cell with optical tweezers. Biol Cell 2006;98:679–95.
[43] Ou-Yang HD, Wei M-T. Complex fluids: probing mechanical properties of biological systems with optical tweezers. Annu Rev Phys Chem 2010;61:421–40.
[44] Moffitt JR, Chemla YR, Smith SB, Bustamante C. Recent advances in optical tweezers. Annu Rev Biochem 2008;77:205–28.
[45] Woerdemann M, Alpmann C, Esseling M, Denz C. Advanced optical trapping by complex beam shaping. Laser Photonics Rev 2013;7:839–54.
[46] Molloy JE, Padgett MJ. Lights, action: optical tweezers. Contemp Phys 2002;43:241–58.
[47] Rohrbach A, Stelzer EHK. Trapping forces, force constants, and potential depths for dielectric spheres in the presence of spherical aberrations. Appl Opt 2002;41:2494–507.
[48] Barton JP, Alexander DR, Schaub SA. Internal and near-surface electromagnetic fields for a spherical particle irradiated by a focused laser beam. J Appl Phys 1988;64:1632–9.
[49] Gouesbet G, Grehan G. Generalized Lorenz-Mie theories, from past to future. Atomization and Sprays 2000;10:277–333.
[50] Bui AAM, Kashchuk AV, Balanant MA, Nieminen TA, Rubinsztein-Dunlop H, Stilgoe AB. Calibration of force detection for arbitrarily shaped particles in optical tweezers. Sci Rep 2018;8:10798.
[51] Bui AAM, Stilgoe AB, Nieminen TA, Rubinsztein-Dunlop H. Calibration of nonspherical particles in optical tweezers using only position measurement. Opt Lett 2013;38:1244–6.
[52] Brzobohatý O, Šiler M, Trojek J, Chvátal L, Karásek V, Zemánek P. Non-spherical gold nanoparticles trapped in optical tweezers: shape matters. Opt Express 2015;23:8179–89.
[53] Almaas E, Brevik I. Radiation forces on a micrometer-sized sphere in an evanescent field. J Opt Soc Am B 1995;12:2429–38.
[54] Barton JP, Alexander DR, Schaub SA. Theoretical determination of net radiation force and torque for a spherical particle illuminated by a focused laser beam. J Appl Phys 1989;66:4594–602.
[55] Ren KF, Gréha G, Gouesbet G. Radiation pressure forces exerted on a particle arbitrarily located in a Gaussian beam by using the generalized Lorenz-Mie theory, and associated resonance effects. Opt Commun 1994;108:343–54.
[56] David SB, David LA. Manipulating particles with light: radiation and gradient forces. Eur J Phys 2017;38:034008.
[57] Pang Y, Gordon R. Optical trapping of a single protein. Nano Lett 2012;12:402–6.

[58] Arita Y, Mazilu M, Dholakia K. Laser-induced rotation and cooling of a trapped microgyroscope in vacuum. Nat Commun 2013;4:2374.
[59] Phillips DB, Padgett MJ, Hanna S, et al. Shape-induced force fields in optical trapping. Nat Photonics 2014;8:400.
[60] Pierini F, Zembrzycki K, Nakielski P, Pawłowska S, Kowalewski TA. Atomic force microscopy combined with optical tweezers (AFM/OT). Meas Sci Technol 2016;27:025904.
[61] Lang MJ, Fordyce PM, Block SM. Combined optical trapping and single-molecule fluorescence. J Biol 2003;2:6.
[62] Comstock MJ, Whitley KD, Jia H, et al. Direct observation of structure-function relationship in a nucleic acid-processing enzyme. Science 2015;348:352.
[63] Wang Y, Botvinick EL, Zhao Y, et al. Visualizing the mechanical activation of Src. Nature 2005;434:1040–5.
[64] Block SM, Blair DF, Berg HC. Compliance of bacterial flagella measured with optical tweezers. Nature 1989;338:514.
[65] Ashkin A, Schütze K, Dziedzic JM, Euteneuer U, Schliwa M. Force generation of organelle transport measured *in vivo* by an infrared laser trap. Nature 1990;348:346.
[66] Stokes GG. On the effect of the internal friction of fluids on the motion of pendulums. Trans Camb Philos Soc 1850;9:8–106.
[67] Sato S, Ohyumi M, Shibata H, Inaba H, Ogawa Y. Optical trapping of small particles using a 1.3-μm compact InGaAsP diode laser. Opt Lett 1991;16:282–4.
[68] Wright WH, Sonek GJ, Berns MW. Parametric study of the forces on microspheres held by optical tweezers. Appl Opt 1994;33:1735–48.
[69] Khatibzadeh N, Stilgoe AB, Bui AAM, et al. Determination of motility forces on isolated chromosomes with laser tweezers. Sci Rep 2014;4:6866.
[70] Clercx HJH, Schram PPJM. Brownian particles in shear flow and harmonic potentials: a study of long-time tails. Phys Rev A 1992;46:1942–50.
[71] Svoboda K, Block SM. Optical trapping of metallic Rayleigh particles. Opt Lett 1994;19:930–2.
[72] Berg-Sørensen K, Flyvbjerg H. Power spectrum analysis for optical tweezers. Rev Sci Instrum 2004;75:594–612.
[73] Berg-Sørensen K, Peterman EJG, Weber T, Schmidt CF, Flyvbjerg H. Power spectrum analysis for optical tweezers. II: Laser wavelength dependence of parasitic filtering, and how to achieve high bandwidth. Rev Sci Instrum 2006;77:063106.
[74] Landau LD, Lifshitz EM. Fluid Mechanics. Pergamon Press, Oxford, 1987.
[75] Li T, Kheifets S, Medellin D, Raizen MG. Measurement of the instantaneous velocity of a Brownian particle. Science 2010;328:1673.
[76] Kheifets S, Simha A, Melin K, Li T, Raizen MG. Observation of Brownian motion in liquids at short times: instantaneous velocity and memory loss. Science 2014;343:1493.
[77] Gittes F, Schmidt CF. Interference model for back-focal-plane displacement detection in optical tweezers. Opt Lett 1998;23:7–9.
[78] Denk W, Webb WW. Optical measurement of picometer displacements of transparent microscopic objects. Appl Opt 1990;29:2382–91.
[79] Svoboda K, Block SM. Force and velocity measured for single kinesin molecules. Cell 1994;77:773–84.
[80] Czerwinski F, Richardson AC, Oddershede LB. Quantifying noise in optical tweezers by Allan variance. Opt Express 2009;17:13255–69.
[81] Shamir M, Bar-On Y, Phillips R, Milo R. SnapShot: timescales in cell biology. Cell 2016;164:1302–02.e1301.
[82] Phillips R, Kondev J, Theriot J, Garcia H. Physical biology of the cell. Garland Science, New York, 2009.
[83] Jannasch A, Demirörs AF, van Oostrum PDJ, van Blaaderen A, Schäffer E. Nanonewton optical force trap employing anti-reflection coated, high-refractive-index titania microspheres. Nat Photonics 2012;6:469.
[84] Smith SB, Cui Y, Bustamante C. Overstretching B-DNA: the elastic response of individual double-stranded and single-stranded DNA molecules. Science 1996;271:795.
[85] Smith SB, Cui Y, Bustamante C. Optical-trap force transducer that operates by direct measurement of light momentum. In: Methods in Enzymology. Volume 361. San Diego, USA, Academic Press, 2003:134–62.
[86] Farré A, Marsà F, Montes-Usategui M. Optimized back-focal-plane interferometry directly measures forces of optically trapped particles. Opt Express 2012;20:12270–91.
[87] Català F, Marsà F, Montes-Usategui M, Farré A, Martín-Badosa E. Extending calibration-free force measurements to optically-trapped rod-shaped samples. Sci Rep 2017;7:42960.
[88] Pralle A, Prummer M, Florin EL, et al. Three-dimensional high-resolution particle tracking for optical tweezers by forward scattered light. Microsc Res Technol 1999;44:378–86.
[89] Rohrbach A, Stelzer EHK. Optical trapping of dielectric particles in arbitrary fields. J Opt Soc Am A 2001;18:839–53.
[90] Rohrbach A, Tischer C, Neumayer D, Florin E-L, Stelzer EHK. Trapping and tracking a local probe with a photonic force microscope. Rev Sci Instrum 2004;75:2197–210.
[91] O'Neil AT, MacVicar I, Allen L, Padgett MJ. Intrinsic and extrinsic nature of the orbital angular momentum of a light beam. Phys Rev Lett 2002;88:053601.
[92] Barnett SM, Babiker M, Padgett MJ. Optical orbital angular momentum. Phil Trans R Soc A 2017;375:20150444.
[93] Berkhout GCG, Lavery MPJ, Courtial J, Beijersbergen MW, Padgett MJ. Efficient sorting of orbital angular momentum states of light. Phys Rev Lett 2010;105:153601.
[94] Asavei T, Loke VLY, Barbieri M, Nieminen TA, Heckenberg NR, Rubinsztein-Dunlop H. Optical angular momentum transfer to microrotors fabricated by two-photon photopolymerization. N J Phys 2009;11:093021.
[95] Friese MEJ, Enger J, Rubinsztein-Dunlop H, Heckenberg NR. Optical angular-momentum transfer to trapped absorbing particles. Phys Rev A 1996;54:1593–6.
[96] Friese MEJ, Nieminen TA, Heckenberg NR, Rubinsztein-Dunlop H. Optical alignment and spinning of laser-trapped microscopic particles. Nature 1998;394:348.
[97] Bishop AI, Nieminen TA, Heckenberg NR, Rubinsztein-Dunlop H. Optical application and measurement of torque on microparticles of isotropic nonabsorbing material. Phys Rev A 2003;68:033802.
[98] Tong L, Miljković VD, Käll M. Alignment, rotation, and spinning of single plasmonic nanoparticles and nanowires using polarization dependent optical forces. Nano Lett 2010;10:268–73.
[99] La Porta A, Wang MD. Optical torque wrench: angular trapping, rotation, and torque detection of quartz microparticles. Phys Rev Lett 2004;92:190801.
[100] Bishop AI, Nieminen TA, Heckenberg NR, Rubinsztein-Dunlop H. Optical microrheology using rotating laser-trapped particles. Phys Rev Lett 2004;92:198101–4.

[101] Galajda P, Ormos P. Complex micromachines produced and driven by light. Appl Phys Lett 2001;78:249–51.
[102] Quake SR, Babcock H, Chu S. The dynamics of partially extended single molecules of DNA. Nature 1997;388:151.
[103] Deufel C, Forth S, Simmons CR, Dejgosha S, Wang MD. Nanofabricated quartz cylinders for angular trapping: DNA supercoiling torque detection. Nat Methods 2007;4:223–6.
[104] Nieminen TA, Heckenberg NR, Rubinsztein-Dunlop H. Optical measurement of microscopic torques. J Mod Opt 2001;48:405–13.
[105] Parkin S, Knüner G, Nieminen TA, Heckenberg NR, Rubinsztein-Dunlop H. Measurement of the total optical angular momentum transfer in optical tweezers. Opt Express 2006;14:6963–70.
[106] Zhang S, Gibson LJ, Stilgoe AB, Favre-Bulle IA, Nieminen TA, Rubinsztein-Dunlop H. Ultrasensitive rotating photonic probes for complex biological systems. Optica 2017;4:1103–8.
[107] Blehm BH, Devine A, Staunton JR, Tanner, K. *In vivo* tissue has non-linear rheological behavior distinct from 3D biomimetic hydrogels, as determined by AMOTIV microscopy. Biomaterials 2016;83:66–78.
[108] Dzementsei AF, Barooji YA, Ober EB. Oddershede LB. *In vivo* quantification of biomechanical cell properties within deep tissues. Dev Cell 2018.
[109] Asbury CL, Fehr AN, Block SM. Kinesin moves by an asymmetric hand-over-hand mechanism. Science 2003;302:2130–4.
[110] Block SM, Asbury CL, Shaevitz JW, Lang MJ. Probing the kinesin reaction cycle with a 2D optical force clamp. Proc Natl Acad Sci USA 2003;100:2351–6.
[111] Dumont S, Cheng W, Serebrov V, et al. RNA translocation and unwinding mechanism of HCV NS3 helicase and its coordination by ATP. Nature 2006;439:105.
[112] Knight AE, Veigel C, Chambers C, Molloy JE. Analysis of single-molecule mechanical recordings: application to acto-myosin interactions. Prog Biophys Mol Biol 2001;77:45–72.
[113] Mallik R, Carter BC, Lex SA, King SJ, Gross SP. Cytoplasmic dynein functions as a gear in response to load. Nature 2004;427:649.
[114] Pease PJ, Levy O, Cost GJ, et al. Sequence-directed DNA translocation by purified FtsK. Science (NY) 2005;307:586–90.
[115] Ryu WS, Berry RM, Berg HC. Torque-generating units of the flagellar motor of *Escherichia coli* have a high duty ratio. Nature 2000;403:444–7.
[116] Swank DM, Bartoo ML, Knowles AF, et al. Alternative exon-encoded regions of *Drosophila* myosin heavy chain modulate ATPase rates and actin sliding velocity. J Biol Chem 2001;276:15117–24.
[117] Spudich JA, Rice SE, Rock RS, Purcell TJ, Warrick HM. Optical traps to study properties of molecular motors. Cold Spring Harb Prot 2011;2011:1305–18.
[118] Bustamante C, Bryant Z, Smith SB. Ten years of tension: single-molecule DNA mechanics. Nature 2003;421:423.
[119] Cecconi C, Shank EA, Bustamante C, Marqusee S. Direct observation of the three-state folding of a single protein molecule. Science 2005;309:2057–60.
[120] Litvinov RI, Bennett JS, Weisel JW, Shuman H. Multi-step fibrinogen binding to the integrin (alpha)IIb(beta)3 detected using force spectroscopy. Biophys J 2005;89:2824–34.
[121] Thoumine O, Kocian P, Kottelat A, Meister JJ. Short-term binding of fibroblasts to fibronectin: optical tweezers experiments and probabilistic analysis. Eur Biophys J 2000;29:398–408.
[122] Huisstede JH, Subramaniam V, Bennink ML. Combining optical tweezers and scanning probe microscopy to study DNA-protein interactions. Microsc Res Techn 2007;70:26–33.
[123] Svoboda K, Schmidt CF, Schnapp BJ, Block SM. Direct observation of kinesin stepping by optical trapping interferometry. Nature 1993;365:721.
[124] Kuo SC, Sheetz MP. Force of single kinesin molecules measured with optical tweezers. Science (NY) 1993;260:232–4.
[125] Minamino T, Imada K. The bacterial flagellar motor and its structural diversity. Trends Microbiol 2015;23:267–74.
[126] Berg HC. The rotary motor of bacterial flagella. Annu Rev Biochem 2003;72:19–54.
[127] Kojima S, Blair DF. The bacterial flagellar motor: structure and function of a complex molecular machine. In: International Review of Cytology. Volume 233. San Diego, USA, Academic Press, 2004:93–134.
[128] Berry RM, Berg HC. Absence of a barrier to backwards rotation of the bacterial flagellar motor demonstrated with optical tweezers. Proc Natl Acad Sci USA 1997;94:14433–7.
[129] Darnton NC, Berg HC. Force-extension measurements on bacterial flagella: triggering polymorphic transformations. Biophys J 2007;92:2230–6.
[130] Calladine CR. Construction of bacterial flagella. Nature 1975;255:121.
[131] Calladine CR. Change of waveform in bacterial flagella: the role of mechanics at the molecular level. J Mol Biol 1978;118:457–79.
[132] Dogterom M, Yurke B. Measurement of the force-velocity relation for growing microtubules. Science 1997;278:856–60.
[133] Bennink ML, Leuba SH, Leno GH, Zlatanova J, de Grooth BG, Greve J. Unfolding individual nucleosomes by stretching single chromatin fibers with optical tweezers. Nat Struct Biol 2001;8:606.
[134] Bockelmann U, Thomen P, Essevaz-Roulet B, Viasnoff V, Heslot F. Unzipping DNA with optical tweezers: high sequence sensitivity and force flips. Biophys J 2002;82:1537–53.
[135] Keyser UF, Does Jvd, Dekker C, Dekker NH. Optical tweezers for force measurements on DNA in nanopores. Rev Sci Instrum 2006;77:105105.
[136] Perkins T, Quake S, Smith D, Chu S. Relaxation of a single DNA molecule observed by optical microscopy. Science 1994;264:822–6.
[137] Wang MD, Yin H, Landick R, Gelles J, Block SM. Stretching DNA with optical tweezers. Biophys J 1997;72:1335–46.
[138] Zhuang X. Unraveling DNA condensation with optical tweezers. Science 2004;305:188–90.
[139] Liu S, Chistol G, Hetherington CL, et al. A viral packaging motor varies its DNA rotation and step size to preserve subunit coordination as the capsid fills. Cell 2014;157:702–13.
[140] Yurke B, Turberfield AJ, Mills AP Jr, Simmel FC, Neumann JL. A DNA-fuelled molecular machine made of DNA. Nature 2000;406:605–8.
[141] Yan H, Zhang X, Shen Z, Seeman NC. A robust DNA mechanical device controlled by hybridization topology. Nature 2002;415:62–5.
[142] Mao C, Sun W, Shen Z, Seeman NC. A nanomechanical device based on the B-Z transition of DNA. Nature 1999;397:144–6.

[143] Seeman NC, Sleiman HF. DNA nanotechnology. Nat Rev Mater 2017;3:17068.
[144] Leitz G, Greulich KO, Schnepf E. Displacement and return movement of chloroplasts in the marine dinophyte *Pyrocystis noctiluca*. Experiments with optical tweezers. Botanica Acta 1994;107:90–4.
[145] Bayoudh S, Mehta M, Rubinsztein-Dunlop H, Heckenberg NR, Critchley C. Micromanipulation of chloroplasts using optical tweezers. J Microsc 2001;203:214–22.
[146] Berns MW, Aist JR, Wright WH, Liang H. Optical trapping in animal and fungal cells using a tunable, near-infrared titanium-sapphire laser. Exp Cell Res 1992;198:375–8.
[147] Bolognesi G, Friddin MS, Salehi-Reyhani A, et al. Sculpting and fusing biomimetic vesicle networks using optical tweezers. Nat Commun 2018;9:1882.
[148] Hosokawa C, Kudoh SN, Kiyohara A, Taguchi T. Optical trapping of synaptic vesicles in neurons. Appl Phys Lett 2011;98:163705.
[149] Sacconi L, Tolic-Norrelykke IM, Stringari C, Antolini R, Pavone FS. Optical micromanipulations inside yeast cells. Appl Opt 2005;44:2001–7.
[150] Welte MA, Gross SP, Postner M, Block SM, Wieschaus EF. Developmental regulation of vesicle transport in *Drosophila* embryos: forces and kinetics. Cell 1998;92:547–57.
[151] Chan YH, Boxer SG. Model membrane systems and their applications. Curr Opin Chem Biol 2007;11:581–7.
[152] Rumiana D, Said A, Natalya B, Vesselin N, Karin AR, Reinhard L. A practical guide to giant vesicles. Probing the membrane nanoregime via optical microscopy. J Phys Condens Matter 2006;18:S1151.
[153] Dimova R, Pouligny B, Dietrich C. Pretransitional effects in dimyristoylphosphatidylcholine vesicle membranes: optical dynamometry study. Biophys J 2000;79:340–56.
[154] Buican TN, Smyth MJ, Crissman HA, Salzman GC, Stewart CC, Martin JC. Automated single-cell manipulation and sorting by light trapping. Appl Opt 1987;26:5311–6.
[155] Herzenberg LA, Parks D, Sahaf B, Perez O, Roederer M, Herzenberg LA. The history and future of the fluorescence activated cell sorter and flow cytometry: a view from Stanford. Clin Chem 2002;48:1819–27.
[156] Wang MM, Tu E, Raymond DE, et al. Microfluidic sorting of mammalian cells by optical force switching. Nat Biotechnol 2004;23:83.
[157] Schmitz B, Radbruch A, Kummel T, et al. Magnetic activated cell sorting (MACS) – a new immunomagnetic method for megakaryocytic cell isolation: comparison of different separation techniques. Eur J Haematol 1994;52:267–75.
[158] Grover SC, Skirtach AG, Gauthier RC, Grover CP. Automated single-cell sorting system based on optical trapping. J Biomed Opt 2001;6:14–22.
[159] Eriksson E, Scrimgeour J, Granéli A, et al. Optical manipulation and microfluidics for studies of single cell dynamics. J Opt A Pure Appl Opt 2007;9:S113.
[160] Dholakia K, MacDonald MP, Zemanek P, Cizmar T. Cellular and colloidal separation using optical forces. Methods Cell Biol 2007;82:467–95.
[161] Imasaka T, Kawabata Y, Kaneta T, Ishidzu Y. Optical chromatography. Anal Chem 1995;67:1763–5.
[162] MacDonald MP, Spalding GC, Dholakia K. Microfluidic sorting in an optical lattice. Nature 2003;426:421.
[163] Chattopadhyay S, Moldovan R, Yeung C, Wu XL. Swimming efficiency of bacterium *Escherichia coli*. Proc Natl Acad Sci USA 2006;103:13712–7.
[164] Lowe G, Meister M, Berg HC. Rapid rotation of flagellar bundles in swimming bacteria. Nature 1987;325:637.
[165] Darnton NC, Turner L, Rojevsky S, Berg HC. On torque and tumbling in swimming *Escherichia coli*. J Bacteriol 2007;189:1756–64.
[166] Amstrong D, Nieminen TA, Favre-Bulle IA, et al. Direct force measurements of optically trapped *Escherichia coli* in viscous media. In preparation 2019.
[167] Kashchuk A. Measurement of forces in optical tweezers with applications in biological systems. In: School of Mathematics and Physics, Volume Doctor of Philosophy. Brisbane, Australia, The University of Queensland, 2019.
[168] Cordova JC, Das DK, Manning HW, Lang MJ. Combining single-molecule manipulation and single-molecule detection. Curr Opin Struct Biol 2014;28:142–8.
[169] Kellermayer MS. Visualizing and manipulating individual protein molecules. Physiol Meas 2005;26:R119–53.
[170] Xie C, Mace J, Dinno MA, et al. Identification of single bacterial cells in aqueous solution using confocal laser tweezers Raman spectroscopy. Anal Chem 2005;77:4390–7.
[171] Grier DG. A surprisingly attractive couple. Nature 1998;393:621.
[172] Liesener J, Reicherter M, Haist T, Tiziani HJ. Multi-functional optical tweezers using computer-generated holograms. Opt Commun 2000;185:77–82.
[173] Gong Z, Pan Y-L, Videen G, Wang C. Optical trapping-Raman spectroscopy (OT-RS) with embedded microscopy imaging for concurrent characterization and monitoring of physical and chemical properties of single particles. Anal Chim Acta 2018;1020:86–94.
[174] Snook RD, Harvey TJ, Correia Faria E, Gardner P. Raman tweezers and their application to the study of singly trapped eukaryotic cells. Integr Biol 2009;1:43–52.
[175] Ramser K, Logg K, Goksor M, Enger J, Kall M, Hanstorp D. Resonance Raman spectroscopy of optically trapped functional erythrocytes. J Biomed Opt 2004;9:593–600.
[176] Svedberg F, Li Z, Xu H, Käll M. Creating hot nanoparticle pairs for surface-enhanced Raman spectroscopy through optical manipulation. Nano Lett 2006;6:2639–41.
[177] Favre-Bulle IA, Preece D, Nieminen TA, Heap LA, Scott EK, Rubinsztein-Dunlop H. Scattering of sculpted light in intact brain tissue, with implications for optogenetics. Sci Rep 2015;5:11501.
[178] Harlepp S, Thalmann F, Follain G, Goetz JG. Hemodynamic forces can be accurately measured *in vivo* with optical tweezers. Mol Biol Cell 2017;28:3252–60.
[179] Johansen PL, Fenaroli F, Evensen L, Griffiths G, Koster G. Optical micromanipulation of nanoparticles and cells inside living zebrafish. Nat Commun 2016;7:10974.
[180] Vanwalleghem GC, Ahrens MB, Scott EK. Integrative whole-brain neuroscience in larval zebrafish. Curr Opin Neurobiol 2018;50:136–45.
[181] Simmich J, Staykov E, Scott E. Zebrafish as an appealing model for optogenetic studies. Prog Brain Res 2012;196:145–62.
[182] Jun Y, Tripathy SK, Narayanareddy BRJ, Mattson-Hoss MK, Gross SP. Calibration of optical tweezers for *in vivo* force

measurements: how do different approaches compare? Biophys J 2014;107:1474–84.
[183] Kokhanovsky AA. Light scattering reviews. Springer, Berlin/Heidelberg, 2006.
[184] Cheong WF, Prahl SA, Welch AJ. A review of the optical properties of biological tissues. IEEE J Quant Electron 1990;26:2166–85.
[185] Schurr JM, Schmitz KS. Dynamic light scattering studies of biopolymers: effects of charge, shape, and flexibility. Annu Rev Phys Chem 1986;37:271–305.
[186] Stetefeld J, McKenna SA, Patel TR. Dynamic light scattering: a practical guide and applications in biomedical sciences. Biophys Rev 2016;8:409–27.
[187] Dholakia K, Čižmár T. Shaping the future of manipulation. Nat Photonics 2011;5:335.
[188] Mosk AP, Lagendijk A, Lerosey G, Fink M. Controlling waves in space and time for imaging and focusing in complex media. Nat Photonics 2012;6:283.
[189] Gerchberg RW, Saxton OA. A practical algorithm for the determination of phase from image and diffraction plane pictures. Optik 1972;35:237–46.
[190] Reicherter M, Haist T, Wagemann EU, Tiziani HJ. Optical particle trapping with computer-generated holograms written on a liquid-crystal display. Opt Lett 1999;24:608–10.
[191] Accanto N, Molinier C, Tanese D, et al. Multiplexed temporally focused light shaping for high-resolution multi-cell targeting. Optica 2018;5:1478–91.
[192] Leshem B, Hernandez O, Papagiakoumou E, Emiliani V, Oron D. When can temporally focused excitation be axially shifted by dispersion? Opt Express 2014;22:7087–98.
[193] Jordan P, Leach J, Padgett M, et al. Creating permanent 3D arrangements of isolated cells using holographic optical tweezers. Lab Chip 2005;5:1224–8.
[194] Ronzitti E, Ventalon C, Canepari M, Forget BC, Papagiakoumou E, Emiliani V. Recent advances in patterned photostimulation for optogenetics. J Opt 2017;19:113001.
[195] Packer AM, Roska B, Häusser M. Targeting neurons and photons for optogenetics. Nat Neurosci 2013;16:805.
[196] Whyte G, Courtial J. Experimental demonstration of holographic three-dimensional light shaping using a Gerchberg-Saxton algorithm. N J Phys 2005;7:117.
[197] Čižmár T, Mazilu M, Dholakia K. *In situ* wavefront correction and its application to micromanipulation. Nat Photonics 2010;4:388.
[198] Čižmár T, Dalgarno HIC, Ashok PC, Gunn-Moore FJ, Dholakia K. Optical aberration compensation in a multiplexed optical trapping system. J Opt 2011;13:044008.
[199] Horstmeyer R, Ruan H, Yang C. Guidestar-assisted wavefront-shaping methods for focusing light into biological tissue. Nat Photonics 2015;9:563.
[200] Blochet B, Bourdieu L, Gigan S. Focusing light through dynamical samples using fast continuous wavefront optimization. Opt Lett 2017;42:4994–7.
[201] Kirkham GR, Britchford E, Upton T, et al. Precision assembly of complex cellular microenvironments using holographic optical tweezers. Sci Rep 2015;5:8577.
[202] Perez-Castillejos R. Replication of the 3D architecture of tissues. Mater Today 2010;13:32–41.
[203] Akselrod GM, Timp W, Mirsaidov U, et al. Laser-guided assembly of heterotypic three-dimensional living cell microarrays. Biophys J 2006;91:3465–73.
[204] Favre-Bulle IA, Stilgoe AB, Rubinsztein-Dunlop H, Scott EK. Optical trapping of otoliths drives vestibular behaviours in larval zebrafish. Nat Commun 2017;8:630.
[205] Favre-Bulle IA, Vanwalleghem G, Taylor MA, Rubinsztein-Dunlop H, Scott EK. Cellular-resolution imaging of vestibular processing across the larval zebrafish brain. Curr Biol 2018;28:3711–22.e3713.
[206] Mo W, Chen F, Nechiporuk A, Nicolson TJBN. Quantification of vestibular-induced eye movements in zebrafish larvae. BMC Neurosci 2010;11:110.
[207] Migault G, van der Plas TL, Trentesaux H, et al. Whole-brain calcium imaging during physiological vestibular stimulation in larval zebrafish. Curr Biol 2018;28:3723–35.e3726.
[208] Cullen KE. The vestibular system: multimodal integration and encoding of self-motion for motor control. Trends Neurosci 2012;35:185–96.